

6. Sutherland, R. L., *Handbook of Nonlinear Optics*, Marcel Dekker, New York, 1996.
7. Vijaya, R., Murti, Y. V. G. S., Vijayaraj, T. A. and Sundararajan, G., Optical limiting action in poly(para-methoxy phenylacetylene). *Curr. Sci.*, 1997, **72**, 507–508.
8. Liu, C., Zeng, H., Segawa, Y. and Kira, M., Optical limiting performance of a novel σ - π alternating polymer. *Opt. Commun.*, 1999, **162**, 53–56.
9. Li, C., Liu, C., Li, Q. and Gong, Q., Broadband optical limiting and nonlinear optical absorption properties of a novel hyperbranched conjugated polymer. *Chem. Phys. Lett.*, 2004, **400**, 569–572.
10. Wang, H. *et al.*, Synthesis, light-emitting and optical limiting properties of new donor-acceptor conjugated polymers derived from 3,5-dicyano-2,4,6-trisubstituted pyridine. *React. Funct. Polym.*, 2006, **66**, 993–1002.
11. Yin, S., Xu, H., Su, X., Wu, L., Song, Y. and Tang, B. Z., Preparation and property of soluble azobenzene-containing substitution Poly(1-alkyne)s optical limiting materials. *Dyes Pigm.*, 2007, **75**, 675–680.
12. Guang, S., Yin, S., Xu, H., Zhu, W., Gao, Y. and Song, Y., Synthesis and properties of long conjugated organic optical limiting materials with different π electron conjugation bridge structure. *Dyes Pigm.*, 2007, **73**, 285–291.
13. Xu, H., Jiang, M., Song, Y. and Li, C., Optical limiting of a new substituted polydiacetylene. *Mater. Lett.*, 1996, **27**, 91–94.
14. Sun, Y. P. and Riggs, J. E., Organic and inorganic optical limiting materials from fullerenes and nanoparticles. *Int. Rev. Phys. Chem.*, 1999, **18**, 43–90.
15. Sun, W. F., Bader, M. M. and Carvalho T., Third-order optical nonlinearities of α , ω -dihienylpolyenes and oligo(thienylvinylene). *Opt. Commun.*, 2003, **215**, 185–190.

ACKNOWLEDGEMENTS. We thank Prof. I. Othman, the Director General and Head, Department of Physics and Prof. T. Yassine, Head, Department of Chemistry for encouragement and support. We also thanks Dr M. D. Zidan for providing facilities and for valuable discussions and Prof. Isam Marawi, Arab International University for reviewing the work.

Received 16 December 2007; revised accepted 22 May 2008

Single-pulse chemical shock tube for ignition delay measurements

M. Nagaboopathy¹, C. Vijayanand²,
Gopalkrishna Hegde¹, K. P. J. Reddy¹ and
E. Arunan^{2,*}

¹Department of Aerospace Engineering,

²Department of Inorganic and Physical Chemistry,
Indian Institute of Science, Bangalore 560 012, India

We describe a single-pulse chemical shock tube CST2 established for measuring the reaction rate of chemical reactions and ignition delay for fuels at high temperature along with the procedure for its calibration. The suitability of the facility for measuring the ignition delay is demonstrated by measuring the ignition delay for

the ethane–oxygen gas mixture in the temperature range 1250–1611 K by recording the ignition-induced pressure jump and emission from CH radical simultaneously. The results obtained in the present study compare well with the earlier reported values.

Keywords: Chemical kinetics, ignition delay, reaction rate, shock tube.

ESTIMATION of ignition delay as well as the temperature dependence of rate constants in practical systems such as combustion, explosion and detonation is essential to understand the detailed chemical kinetics of fuels for future scramjet and pulse detonation engines. The demand for such data has increased in recent times due to the enhanced global interest in hypersonic vehicles for military as well as space applications. A shock tube is an ideal tool to measure the kinetics data^{1,2} and ignition delays^{3,4} for the fuels of interest in hypersonic applications which occur at temperatures exceeding 1000 K. In addition, shock tubes have been used in many other fields such as aerodynamics, physics, chemistry, materials science, biology⁵, industrial and medical applications⁶.

Ignition delay time of a fuel is the characteristic time used to scale the duration of the gas flow passing through the combustion chamber. This is an important criterion to measure the capability of ignition and flame sustainance in the engine. Computational fluid dynamics (CFD) is frequently used to simulate the various types of fluid flows and also the real-time chemical processes in a combustion chamber. In order to validate these simulation results it is necessary to have an accurate chemical reaction model. Experimentally measured ignition delay provides one of the important criteria to validate CFD results. Moreover, some suitable additives could be tried in shock-tube experiments which could help in reducing the ignition delay of hydrocarbon fuels before their use in scramjet engines^{7,8}.

We have recently established two chemical shock tubes (CST1 and CST2), at the High Temperature Chemical Kinetics Laboratory of Aerospace Engineering Department⁹ at IISc, which have been extensively used to study the pyrolysis of different molecules^{10,11}. There has been a recent increase in the need for ignition-delay data for fuels used in Scramjet engines, which are being developed in the country to meet the future demands. The ignition-delay data for hydrocarbon fuels with additives and hydrogen are essential for the design of these scramjet engines. In order to meet this demand we have initiated ignition-delay measurement studies by modifying the CST2 shock tube with additional diagnostics¹². The aim of this communication is to describe the chemical shock tube used for ignition-delay measurements and present its performance details along with the preliminary data measured for ethane–oxygen gas mixture using this facility.

*For correspondence. (e-mail: arunan@ipc.iisc.ernet.in)

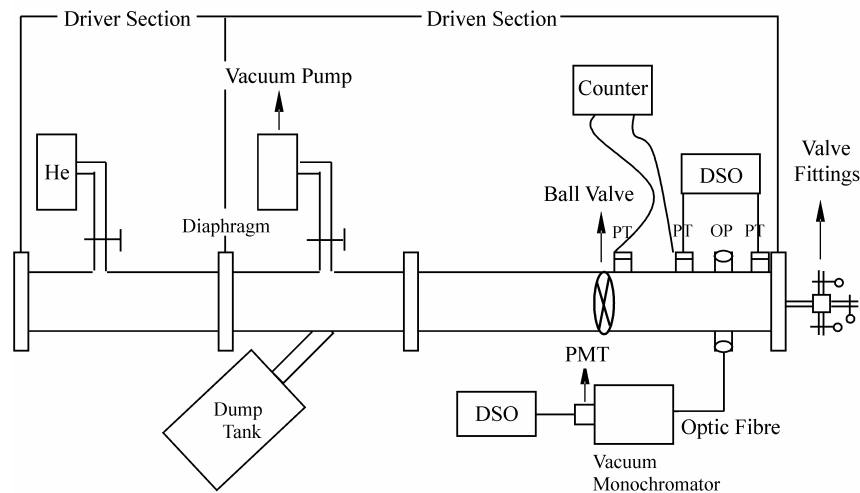


Figure 1. Schematic diagram of the chemical shock tube, CST2. DSO, Digital storage oscilloscope (Tektronix, TDS 210); PT, Pressure transducers (PCB model 113A24); OP, Optical ports; Counter, HP 5314A universal counter; PMT, Photo-multiplier tube.

The CST2 shock tube (Figure 1) is a 39 mm internal diameter, SS314-grade, stainless-steel tube divided into driver and driven sections separated by a metallic diaphragm. The 197 cm long driver section is provided with instrumentation ports for connecting the high-pressure gas cylinders, pressure gauges, vent line and vacuum pumps. Similarly, the 441 cm long driven section is also provided with ports for connecting the vacuum pumping system, test-gas feeding system, thermal sensors for measuring shock speed and sensors to measure pressure rise behind the primary and reflected shock waves at various locations of the driven section (Figure 1). The shock tube is designed and tested for pressure levels up to 3500 PSI. The typical driven-to-driver section length ratio is above 2, and it can be varied by including additional length of the tube to either the driver or driven sections. The driven section is also provided with a ball valve of 39 mm internal bore, such that the reactant gas is confined only to the region between the ball valve and the end flange of the driven section before the passage of the shock wave. The ball valve is essential to have a well-defined dwell time, as it is commonly referred to in the literature^{9,13}. The end flange is provided with an outlet which can be used to load the reactant samples into the driven section as well as to draw the equilibrated gas after exposure to the shock wave for subsequent product analysis.

Two diagonally opposite ports mounted with provision for optical windows are provided at the end of the driven tube after the ball valve. The light emitted during the chemical reactions induced by the passage of the shock wave through the reactants is collected by the collector optics mounted on one of the ports and sent to the monochromator (Acton model VM502) through a fibre optic bundle (Figure 1). The emitted light signal is recorded by the attached photomultiplier tube (PMT model DA-780-

VUV) connected to a digital storage oscilloscope. The monochromator has the wavelength range of 110–550 nm and the PMT works in the entire range of wavelengths as well. In the current set of experiments, the emission signal was detected by tuning the monochromator to the band centre of the known emission spectrum of CH. The diagonally opposite window can be used to mount a pressure sensor. The arrival of reflected shock at the window gives us the zero time and time-delay before the CH emission signal gives the ignition delay. Both ports can be fitted with appropriate optical windows in case absorption spectroscopy is to be used for monitoring transients produced following shock excitation of the gaseous mixture.

A dump tank is attached to the driven section of the shock tube in the downstream region immediately after the diaphragm station. In the absence of the dump tank, the reflected shock wave from the end of the driven section travels back all the way through the shock tube and gets reflected again by the end flange of the driver section, and returns to the shocked test gas once again to increase its temperature. This keeps repeating a few times, which results in reheating the test sample multiple times with temperature pulses of receding magnitude. This is eliminated by the dump tank downstream of the diaphragm station which swallows the reflected shock and hence the sample is heated by a single, well-defined temperature pulse. However, in the present set of experiments, ignition of the fuel/oxygen mixture is initiated by the reflected shock wave at the end of the driven section. Since the ignition delay is measured well before the secondary reflection from the driver side, the dump tank is not needed in these experiments.

A shock wave is produced by rupturing the aluminium diaphragm which separates the driver and the driven sections, by increasing the He pressure. The driven section is

filled with the required test gas at a typical pressure (P_1) of 200 Torr, the pressure (P_4) at which the diaphragm ruptures is recorded. The pressure rise behind the primary and the reflected shock wave shown in Figure 2 is recorded using a pressure sensor mounted at the end of the driven section. The output signals from the pressure sensors mounted 50 cm apart near the end of the driven section are used to calculate the shock Mach number M_s . From M_s , the pressure P_5 and temperature T_5 resulting from the reflected shock wave can be calculated using the following normal shock relations (Rankine–Hugoniot equation):

$$\frac{P_5}{P_1} = P_{51} = \left[\frac{2\gamma M_s^2 - (\gamma - 1)}{(\gamma + 1)} \right] \left[\frac{(3\gamma - 1)M_s^2 - 2(\gamma - 1)}{(\gamma - 1)^2 M_s^2 + 2} \right], \quad (1)$$

$$\frac{T_5}{T_1} = T_{51} = \frac{[2(\gamma - 1)M_s^2 + (3 - \gamma)][(3\gamma - 1)M_s^2 - 2(\gamma - 1)]}{(\gamma + 1)^2 M_s^2}. \quad (2)$$

Here, T_1 is the temperature of the gas before the arrival of the shock wave and γ is the specific heat ratio of the test gas. If the estimated value of the pressure P_5 from eq. (1) matches well with the corresponding measured value from Figure 2, for a given set of P_4 and P_1 values, the shock tube is performing as expected. The pressure signals from different ports along the driven section can also be used to measure the speed of the shock wave at different points

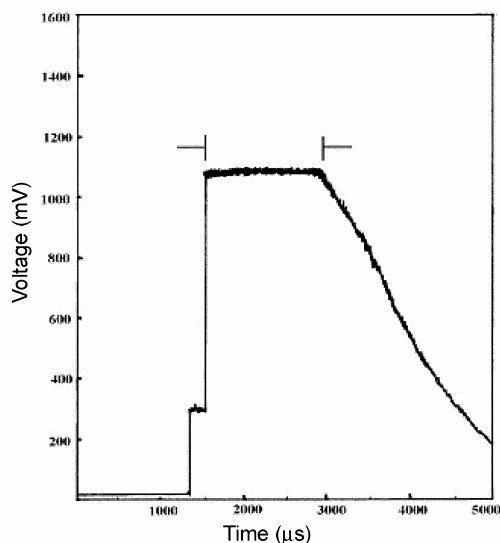


Figure 2. Typical pressure trace showing the arrival of primary shock (first jump) and reflected shock (second jump) waves and dwell time shown. Arrival of the expansion fan at the end of the dwell time quenches the shock-heated mixture, providing a nearly 'single high-temperature pulse'.

and ensure that we have a uniform shockwave in the region of observation, i.e. it is not attenuated/accelerated within the length of the shock tube. From Figure 2, it can be seen that the pressure and temperature following the arrival of reflected wave P_5 is constant for certain time, until the arrival of the expansion fan which quenches the shock-heated gaseous mixture. It follows from Figure 2 and eqs (1) and (2) that the temperature behind the reflected shock, T_5 , will be constant during this period. Thus, in a single-pulse shock tube the reaction rates are measured at P_5 and T_5 . If the sample section has only a single molecule (could be a fuel), its thermal decomposition can be studied under these conditions. An internal standard could be used to calibrate the temperature, if needed^{9–11}. If the sample section is loaded with a fuel–oxygen mixture, ignition can start and one sees a sudden pressure rise following P_5 .

In order to check the suitability of the CST2 shock tube for ignition-delay measurements, combustion of ethane–oxygen gas mixture was investigated over temperatures in the range 1250–1611 K. Studies have shown that the ethane has shorter ignition delay than other linear chain, branched, cyclic and ringed-structure hydrocarbons^{14–24} and it is in the range of submillisecond at this T range. Hence, the length of the shock tube is adjusted to obtain a dwell time of about 1.5 ms. An ethane–oxygen mixture was taken at an equivalence ratio (ϕ) of 1 and diluted with argon for a desired concentration. The gaseous mixture was allowed to mix for 2–3 h in the sample portion between the ball valve and the end of the driven section, to make a homogeneous mixture. The rest of the driven section was filled with argon at the same pressure as the sample pressure. The ball valve was opened fully just before the bursting of the diaphragm. Since the pressure levels on either side of the ball valve were equal, the mixing of the sample gas with argon gas before the arrival of the shock wave is negligible. In all the experiments, both driver and driven portions are pumped down to below 1×10^{-5} mbar prior to the loading of the helium driver gas and the sample gas respectively. Some experiments with equivalence ratio of 0.5 were carried out as well.

The ignition delay was simultaneously measured by using two techniques. The combustion of the ethane–oxygen gas mixture due to heating by the passage of the reflected shock in the sample region enhances the pressure in the region. This rise in pressure recorded by the sensor located in the port opposite the optical port shown in Figure 1, indicates the onset of ignition, and time interval between the starting of P_5 pressure signal and the onset of ignition is the ignition delay. Ignition of all hydrocarbon fuels leads to the production of CH radicals in excited electronic state, which is rapidly quenched. Emission from the electronically excited CH can be observed as an independent measure of ignition delay. The CH emission range extends from 420 to 440 nm, and its high intense first-order emission lies at 431.5 nm. Hence the

monochromator interfaced with shock tube through optical fibre bundle is centred at 431.5 nm wavelength. The CH emission signal from the ignition of ethane–oxygen mixture is recorded in real time using DSO. Figure 3 shows the typical oscilloscope traces for pressure and CH emission

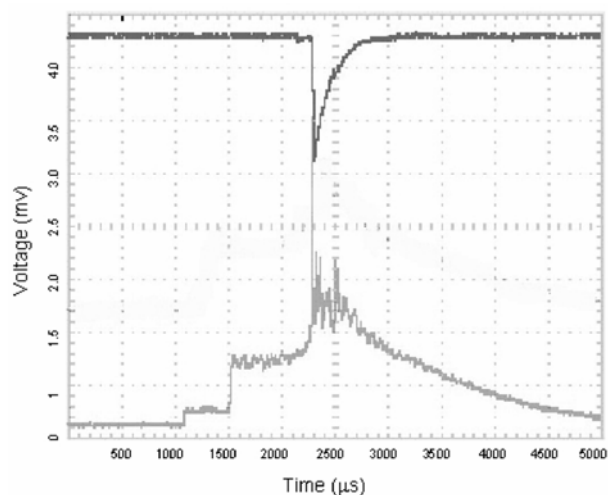


Figure 3. Typical experimental signals recorded showing CH emission (upper trace) and pressure rise (lower trace) for ethane ignition. The time difference between the arrival of the reflected shock (second jump) and the pressure rise/CH emission due to ignition is the ignition delay.

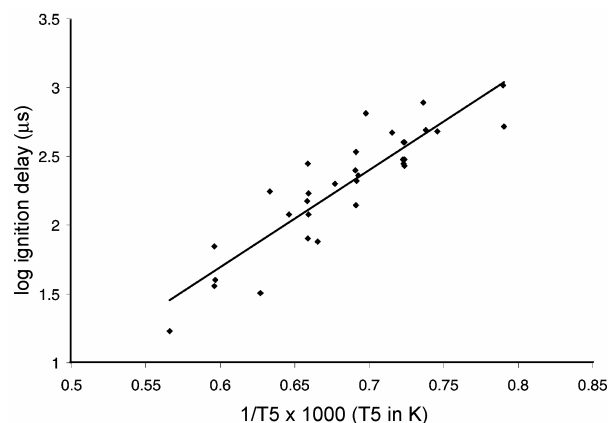


Figure 4. Arrhenius plot for ignition-delay data for $C_2H_6-O_2$ mixture of equivalence ratio 0.5.

Table 1. Arrhenius parameters for ignition-delay data on $C_2H_6-O_2$

ϕ	$T(K)$	$-\log A$	Ea (kcal/mol)	Reference
1.0	1448–1887	4.59	39.6	23
1.0	1204–1700	2.12	31.1	24
1.0	1310–1611	3.26	38.0	Present study
0.5	1448–1887	2.11	31.1	23
0.5	1265–1767	2.54	32.2	Present study

profiles. Here the ignition delay time is defined as the time interval between the arrival of the reflected shock-wave front and the onset of CH emission/pressure rise. Evidently, the ignition-delay time measured from the CH emission is the same as that from the pressure trace, as has been noted earlier by Davidson and Hanson¹⁸. The delay corresponding to this signal is 930 μs at a temperature of 1296 K. The dependence of the ignition-delay time on the temperature and pressure was investigated by performing experiments in the reflected shock mode over a temperature range of 1265–1767 K and pressure range of 8–19 atm. Temperature dependence of ignition delay is usually interpreted using an Arrhenius equation and $\log \tau$ vs $1/T$ plots are linear, if such an approach is reasonable. Figure 4 shows a representative Arrhenius plot for the ignition-delay data for ethane–oxygen of equivalence ratio 0.5. Here the slope is positive, unlike in typical Arrhenius plots of rate constant vs $1/T$, showing a negative slope. Ignition delays decrease with increasing T and the rate constants usually increase with increasing T . From Figure 4, the effective activation energy for C_2H_6 ignition is determined to be 32.2 kcal mol⁻¹. Our experimental results are given in Table 1 along with previous reports on the ignition delay of C_2H_6 . The agreement between our results and the earlier reported results is reasonable giving us confidence in the newly established shock tube facility for ignition delay measurements.

Davidson *et al.*¹⁹ and Oehlschlaeger *et al.*²⁰ studied CH-radical emission from the combustion of jet-propulsion hydrocarbon fuels and various aliphatic hydrocarbons in reflected shock conditions at temperatures in the range of 1177–2009 K and pressure in the range of 1.10–12.58 atm. Their prediction of ignition times and CH, OH concentration time histories are helpful for modelling oxidation mechanisms for seven branched alkanes and serves as a unique database for validating hydrocarbon oxidation mechanisms of propulsion-related fuels. It is planned to use this shock-tube facility for producing ignition delay and chemical kinetic data for fuels of interest to DRDL and ISRO. It is hoped that the results from such investigations will be useful in the ultimate design of hypersonic vehicles.

Chemical shock tube CST2 has been established for measuring the ignition delay for chemical reactions occurring at high temperatures and pressures. The ignition delay can be measured simultaneously by observing the pressure rise in the sample section as well as by monitoring light emission from the CH radicals initiated by the onset of ignition of fuel/oxygen mixture. Experimental data presented here for the ignition of ethane–oxygen mixture demonstrate the capabilities of the shock tube for measuring the ignition delay over a wide range of temperature and pressure. The facility is currently being used to study the ignition delay and chemical kinetics of a high-energy density fuel (JP-10), which is being considered for use in future scramjet and pulse-detonation engines.

1. Tsang, W. and Lifshitz, A., Shock tube techniques in chemical kinetics. *Annu. Rev. Phys. Chem.* 1990, **41**, 559–599.
2. Lifshitz, A. (ed.), *Shock Waves in Chemistry*, Marcell Dekker, New York, 1981.
3. Shin, K. S., Park, K. and Kim, K., The addition effect of CH₃Cl on methane ignition behind reflected shock waves. *Bull. Korean Chem. Soc.*, 2001, **22**, 330–332.
4. Olchansky, E. and Burcat, A., Decane oxidation in a shock tube. *Int. J. Chem. Kinet.*, 2006, **38**, 703–713.
5. Jagadeesh, G., Nataraja, K. N. and Udayakumar, M., Shock waves can enhance bacterial transformation with plasmid DNA. *Curr. Sci.*, 2004, **87**, 734–735.
6. Ben-Dor, G., Igra, O. and Elium, T., *Handbook of Shock Waves, Vols 1–3*, Academic Press, London, 2001.
7. Held, T. J., Marchese, A. J. and Dryer, F. L., A semi-empirical reaction mechanism for *n*-heptane oxidation and pyrolysis. *Combust. Sci. Technol.*, 1997, **123**, 107–146.
8. Li, S. C., Varatharajan, B. and Williams, F. A., Chemistry of JP-10 ignition. *AIAA J.*, 2001, **39**, 2351–2356.
9. Rajakumar, B., Anandraj, D., Reddy, K. P. J. and Arunan, E., Chemical kinetics studies using shock tubes at high temperatures. *J. Indian Inst. Sci.*, 2002, **82**, 37–47.
10. Rajakumar, B., Reddy, K. P. J. and Arunan, E., Unimolecular HCl elimination from 1,2-dichloroethane: A single pulse shock tube and *ab initio* study. *J. Phys. Chem. A*, 2002, **106**, 8366–8373.
11. Rajakumar, B., Reddy, K. P. J. and Arunan, E., Thermal decomposition of 2-fluoroethanol: Single pulse shock tube and *ab initio* studies. *J. Phys. Chem. A*, 2003, **107**, 9782–9793.
12. Nagaboopathy, M. *et al.*, Ignition delay studies on hydrocarbon fuel with and without additives. In Proceedings of the 26 International Symposium on Shock Waves, University of Gottingen, 2007.
13. Tschuikow-Roux, E., Reaction dwell time and cooling rate in single-pulse shock tube. *Phys. Fluids*, 1965, **8**, 821–825.
14. Lamoureux, N., Paillard, C. E. and Vaslier, V., Low hydrocarbon mixtures ignition delay times investigation behind reflected shock waves. *Shock Waves*, 2002, **11**, 309–322.
15. Simmie, J. M., Detailed chemical kinetic models for the combustion of hydrocarbon fuels, *Prog. Energy Combust. Sci.*, 2003, **29**, 599–634.
16. Toland, J. M. Simmie, Ignition of alkyl nitrate/oxygen/argon mixtures in shock waves and comparisons with alkanes and amines. *Combust. Flame*, 2003, **132**, 556–564.
17. Slutsky, V. G., Kazakov, O. D., Severin, E. S., Bespalov, E. V. and Tsyganov, S. A., Self-ignition of small-ring hydrocarbons behind reflected shock waves. *Combust. Flame*, 1993, **94**, 108–112.
18. Davidson, D. F. and Hanson, R. K., Interpreting shock tube ignition data. *Int. J. Chem. Kinet.*, 2004, **36**, 510–523.
19. Davidson, D. F., Horning, D. C. and Hanson, R. K., Shock tube ignition time measurements for *n*-heptane/O₂/Ar and JP-10/O₂/Ar mixtures AIAA paper AIAA-99-2216, 35th Joint Propulsion Conference, Los Angeles, CA, July 1999.
20. Oehlschlaeger, M. A., Davidson, D. F., Herbon, J. T. and Hanson, R. K., Shock tube measurements of branched alkane ignition times and OH concentration time histories. *Int. J. Chem. Kinet.*, 2003, **36**, 67–78.
21. Park, K., Bae, G. T. and Shin, K. S., The addition effect of Fe(CO)₅ on methane ignition. *Bull. Korean Chem. Soc.*, 2002, **23**, 175–176.
22. de Vries, J., Hall, J. M., Simmons, S. L., Rickard, M. J. A., Kalitan, D. M. and Petersen, E. L., Ethane ignition and oxidation behind reflected shock waves. *Combust. Flame*, 2007, **150**, 137–150.
23. Cooke, D. F. and Williams, A., Shock tube studies of methane and ethane oxidation. *Combust. Flame*, 1975, **24**, 245–256.
24. Burcat, A., Scheller, K. and Lifshitz, A., Shock-tube investigation of comparative ignition delay times for C₁–C₅ alkanes. *Combust. Flame*, 1971, **16**, 29–33.

ACKNOWLEDGEMENTS. We thank DRDL Hyderabad; DST, New Delhi and IISc-ISRO Space Technology Cell for financial support. We also thank Mukesh Agarwal, Dinesh Bilehal and D. S. S. Hembram for their preliminary efforts in this work and Dr Amit Pathak and Harish Kumar Chakravarty for helpful discussion.

Received 14 March 2008; revised accepted 11 June 2008

Dynamics of *Anopheles culicifacies*-transmitted malaria in the absence of effective zooprophyllaxis in a riverine settlement in Gujarat, India

R. M. Bhatt^{1,*}, H. C. Srivastava², Rajnikant³ and R. S. Yadav²

¹National Institute of Malaria Research, Field Unit, RLTRI Campus, Raipur 492 015, India

²National Institute of Malaria Research, Field Unit, Civil Hospital, Nadiad 387 001, India

³Indian Council of Medical Research, New Delhi 110 029, India

A study on the bionomics of malaria vector, *Anopheles culicifacies* and its role in malaria transmission was carried out in two phases between August–July 1991–92 and 2000–01 in Galteshwar, a small village situated on the perennial river Mahi, Kheda District, Gujarat, where the ratio of cattle to man was <1, compared to nearly equal or more elsewhere in the district. *An. culicifacies* was the predominant vector species in all collections and was mainly endophilic, though good numbers were also collected outdoors during 1991–92. Its mean human biting rates were 17.4 (1991–92) and 10.7/man/night (2000–01) and varied significantly indoors and outdoors during the hot and rainy seasons, and also between different quarters of the night during the first phase of study. Anthropophilic indices reported as 22.7 and 29.4% in samples collected from human dwellings during both phases were considerably high than reported previously from other parts of the district. The annual entomological inoculation rates estimated for the two study periods varied greatly. Estimates of vectorial capacity for different months during 1991–92 did not correlate with the malaria infection rate in the population. *An. culicifacies* was found resistant to DDT, dieldrin and malathion and the latter was used for indoor residual spraying during the 7-year intervening period. The study showed that the people are at a relatively greater risk of malaria in human settlements like Galteshwar, where there was little opportunity for diversion of mosquitoes to feed on cattle.

*For correspondence. (e-mail: rmbhatt@rediffmail.com)